



A Second Level Trigger for HESS Phase 2

M. Tluczykont, G. Fontaine, M. Ouchrif, J.-C. Prévotet, F. Verdier

► To cite this version:

M. Tluczykont, G. Fontaine, M. Ouchrif, J.-C. Prévotet, F. Verdier. A Second Level Trigger for HESS Phase 2. Towards a Network of Atmospheric Cherenkov Detectors VII, Apr 2005, Palaiseau, France. pp.509-518. in2p3-00127367

HAL Id: in2p3-00127367

<https://hal.in2p3.fr/in2p3-00127367>

Submitted on 29 Jan 2007

HAL is a multi-disciplinary open access archive for the deposit and dissemination of scientific research documents, whether they are published or not. The documents may come from teaching and research institutions in France or abroad, or from public or private research centers.

L'archive ouverte pluridisciplinaire **HAL**, est destinée au dépôt et à la diffusion de documents scientifiques de niveau recherche, publiés ou non, émanant des établissements d'enseignement et de recherche français ou étrangers, des laboratoires publics ou privés.

A Second Level Trigger for H.E.S.S. Phase 2

Martin Tluczykont

Gérard Fontaine

Laboratoire Leprince-Ringuet, École Polytechnique - CNRS/IN2P3 Palaiseau, France

Mohamed Ouchrif

Laboratoire de Physique Nucléaire et de Hautes Energies, IN2P3/CNRS, Universités Paris VI & VII, France

Jean-Christophe Prévotet

Francois Verdier

Université de Cergy-Pontoise, France

After a very successful start with many sources detected, the second phase of the H.E.S.S. experiment is being implemented. The objective is to build a very large telescope in the center of the array of the 4 existing ones. Operating the very large telescope in coincidence (stereoscopy) with the four H.E.S.S. I telescopes allows to reduce the energy threshold from 100 GeV to 50 GeV. In order to make optimum use of this additional very large telescope and to lower the energy threshold further, one has to consider the single telescope events of this telescope as well. The data acquisition of these events requires a second level trigger for the reduction of the data flow. The concepts for the realization and properties for a second level trigger are presented.

1 Introduction

Cherenkov astronomy has entered a new era where not only a few but many sources of different classes are detected and also new classes of sources are found.

The strategy of lowering the energy threshold of Cherenkov telescopes in order to access new source populations was mainly motivated by the fact that many sources were detected up to a few tens of GeV by EGRET [2], whereas the Cherenkov telescopes of the Whipple generation could only access a few sources above 300 GeV. This gap between the highest energies reachable by satellite experiments like GLAST (≈ 100 GeV) and the threshold of Cherenkov telescopes of the current generation like H.E.S.S. Phase I (≈ 100 GeV) is virtually closed. However, for many sources, the

limited sensitivity of GLAST above 100 GeV will probably only allow detections after deep exposures at very high energies. Further, an overlap of good sensitivity over a wider energy range will provide a means of cross-calibrating the two detection techniques. It is therefore planned to lower the energy threshold and to increase the sensitivity of H.E.S.S. at lower energies in the second phase of the experiment, thus effectively closing the gap and also providing an improved overlap in energy between GLAST and H.E.S.S. This will be achieved with an additional very large Cherenkov telescope (VLCT) in the center of the current system. With a reflector diameter of ≈ 28 m the resulting mirror area of the VLCT will amount to roughly 600 m^2 . A camera consisting of 2048 photomultiplier tubes (PMTs) located at 35 m from the reflector, will provide a field of view of 3.5 deg in diameter. One PMT will have a viewing angle of 0.07 deg (as compared to 0.16 deg for H.E.S.S. phase 1). At this conference, an overview of H.E.S.S. phase II was presented by [4] and the camera electronics were presented by [1].

The VLCT will be operated together with the existing large Cherenkov telescopes (LCTs). Stereoscopic events including triggers from at least 2 telescopes out of 5 (4 LCT + 1 VLCT), as well as monoscopic events triggered by the VLCT alone will be recorded by the data acquisition (DAQ) system. Because of the very low energy threshold of the VLCT (≈ 20 GeV, depending on the trigger thresholds of the PMTs) and of its much higher sensitivity at lower energies, three different event classes according to the following (roughly estimated) energy bands, have to be distinguished:

- $E < 50$ GeV: Monoscopic VLCT events
- $50 < E < 100$ GeV: New stereoscopic VLCT/LCT events
- $E > 100$ GeV: Stereoscopic VLCT/LCT events

Between energies around the threshold of the VLCT up to approx. 50 GeV the bulk of the γ -ray showers will only trigger the very large telescope, thus producing monoscopic events. From 50 to 100 GeV many showers that currently (phase 1) only trigger one single LCT (and are thus not taken into account) will, in the phase 2, additionally trigger the VLCT. At these energies most events will therefore be *new stereoscopic events* (VLCT/LCT). Above 100 GeV, many showers will trigger two LCTs and almost all of these events will also trigger the VLCT, providing an additional high resolution image of the shower. This will improve the energy and angular resolution of the detector as compared to phase 1 and will also increase the sensitivity above 100 GeV. Consequently, with one additional central VLCT the overall gain is two-fold: a new energy window will be opened below 100 GeV and the resolution of the detector system will be improved above that energy.

The level-1 (L1) trigger of the VLCT is based on the same principle as the camera trigger of the existing LCTs [5]. Each PMT signal passes a comparator with threshold A_{thr} given in photoelectrons (ph.e.). The L1 trigger condition is fulfilled if in one out

of 96 overlapping sectors (of 64 PMTs each) a minimum number N_S of PMTs has an amplitude above A_{thr} . Depending on the chosen threshold A_{thr} and N_S , a raw L1 trigger rate (estimated from Monte Carlo simulations) for the VLCT of at least 2.5 kHz is expected, reaching up to 20 kHz for the loosest trigger conditions tested. It is desirable to operate the VLCT with the lowest possible PMT thresholds in order to maximize the sensitivity at low energies. The contribution of the four existing LCTs to the total trigger rate, i.e. the transfer rate to the DAQ, is less than 0.5 kHz. In order to avoid transmission and storage of high data rates to the DAQ system the transmission rate has to be limited to a value of the order of 4 kHz. Low PMT thresholds thus require a second level trigger to reduce the transmission rate to the DAQ. Another constraint is that the L1 trigger rate (local camera trigger) has to be less than 50 kHz in order to avoid too high a dead-time.

2 Concept of a Level 2 Trigger

The goal of the second level trigger (subsequently L2) is the optimization of the data flow at optimum detector configuration. The principle of the L2 trigger discussed here is an analysis of camera images built from the available information at the trigger level. In the following subsections, the information used for the L2 trigger and the criteria under study are addressed using Monte Carlo simulations. However, the implementation of a second level trigger will depend on the final design of the camera electronics.

2.1 Image on Trigger Level

In this work it is assumed that the H.E.S.S. Phase II camera pixels are grouped in *blocks* of 2x2 PMTs and one block is an active image element if the number of PMTs above a certain amplitude threshold A_{thr} in the block is $N_{pmt} \geq 2$ (multiplicity). This definition of an image element provides images with binary block-amplitude information (active/inactive, see Figure 1 for illustration). In the simulations carried out for this work, the total amplitude of the L2 image is estimated using three different definitions. Given N_{blocks} , the number of *active blocks* in the image, N_{pmt} , the number of PMTs above threshold in one *block* and the uncalibrated amplitude A_j of PMT j , the *size* S is defined as:

$$S = \sum_{i=0}^{N_{blocks}} \sum_{j=0}^{N_{pmt}} A_j. \quad (1)$$

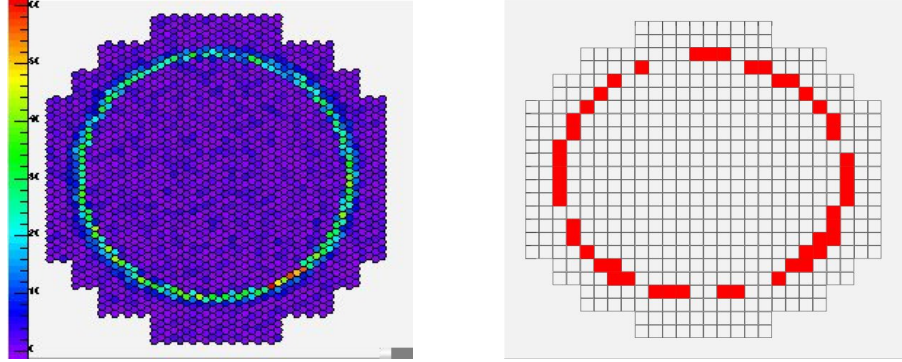
The *pseudo size* is given by

$$PS = \sum_{i=0}^{N_{\text{blocks}}} N_{\text{pmt}}^{(i)}, \quad (2)$$

and finally, the *simple pseudo size* is defined as

$$SPS = N_{\text{blocks}} \quad (3)$$

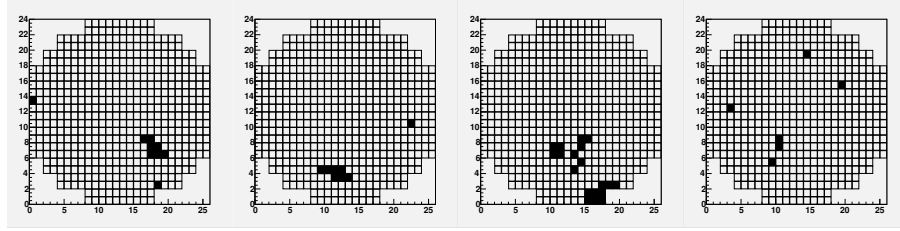
Figure 1: Images of a simulated muon ring event. Left: offline analysis image built from camera pixels with intensities (arbitrary units). Right: image on trigger level built from blocks of 2x2 pixels each. The number of pixels above threshold in one block is at least 2.



2.2 Rejection Criteria on Trigger Level

In Figure 2, images built from the blocks introduced in the previous section are shown for different primary particles species. Some criteria are evident from these images. In Table 1 different possible criteria for the discrimination of γ -like shower events from background are listed. Hillas-type analyses [3] are generally used for the analysis in γ -astronomy with Cherenkov telescopes. The curvature analysis could provide a means of detecting muon rings or arclets in a shower image, clearly identifying the event as of hadronic nature. Hadronic events exhibit a higher image irregularity and more diffuse light distributions than γ -ray induced events.

Figure 2: Images on trigger level using the binary amplitude information . Particle species / event type from left to right: γ , μ (at large impact parameter), hadron, night-sky background.



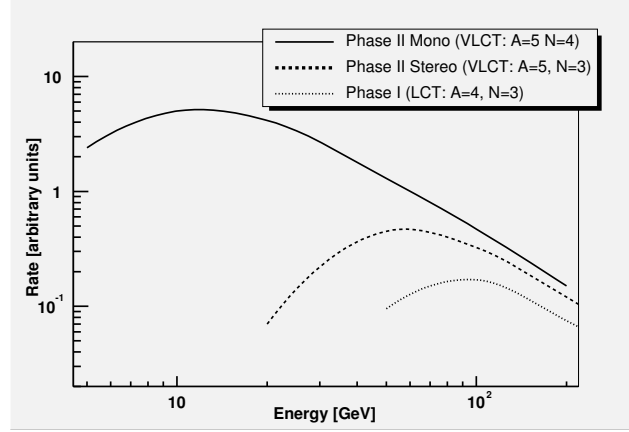
Criterion	Particle species
Hillas-type analyses	All
Curvature analysis	μ 's
Clustering/Irregularity	Hadrons
Isolated Pixels	Night-sky background

Table 1: Rejection criteria for a level 2 (L2) trigger based on image analyses or simple pattern recognition of shower images.

3 Results

The simulations were done using the shower simulator KASKADE and a detector simulation also used in H.E.S.S. phase 1. Electromagnetic showers were produced at discrete energies and with a Crab-Nebula like spectrum. Proton-initiated air showers with a cosmic ray spectrum from energy $E = 5 \text{ GeV}$ to $E = 10 \text{ TeV}$ were simulated over a large parameter space (up to a core impact position of 1000 m, over a field of view of 5°) for the estimation of the hadronic induced trigger rate. An estimation of the differential γ -ray count rate based on these simulations is shown in Figure 3 for monoscopic triggers from the VLCT alone, stereoscopic triggers from hybrid LCT/VLCT triggers and for stereoscopic LCT (phase 1) triggers for comparison. The result for monoscopic events was obtained using the following level 1 (L1) trigger conditions: amplitude threshold $A_{\text{thr}} = 5 \text{ ph.e.}$, sector multiplicity threshold $N_S = 4$. For this configuration, the L1 trigger rate as estimated from simulated proton air showers is 2.5 kHz. This value is well within the specifications for the data transfer limit. The estimated dead-time (local L1 camera trigger) is smaller than 1 % for this rate. Thus, it is possible to reduce the PMT thresholds in order to increase the sensitivity at low energies. Reducing the PMT threshold from $A=5 \text{ ph.e.}$ to $A=3 \text{ ph.e.}$ results in a trigger rate of 5 kHz. The goal of the L2 trigger is to reduce this increased trigger rate in order to keep the transmission rate low. At the same time a high γ -ray efficiency has to be maintained.

Figure 3: Differential L1 γ -ray count rate (arbitrary units) for the H.E.S.S. phase I stereoscopic LCT operation (dotted line), the phase II hybrid (LCT + VLCT) stereo operation (dashed line) and for monoscopic operation of the VLCT (solid line).

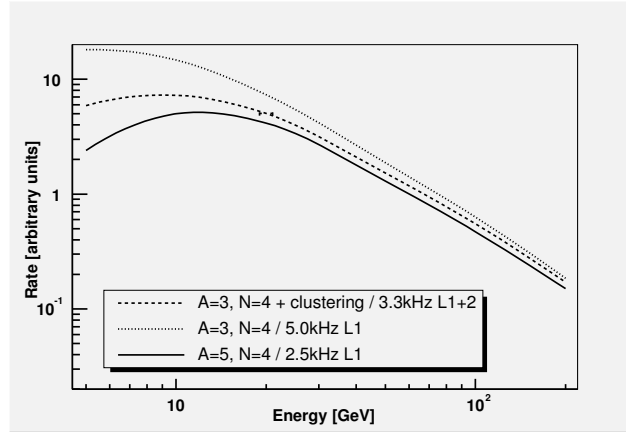


3.1 L2 Clustering Condition

Each block (see section 2.1) is adjacent to 8 next neighbouring blocks. A cluster is defined as a group of at least 2 adjacent active blocks. Shower images are produced by highly directional Cherenkov light emitted by an ensemble of particles produced within the shower. Therefore, the images are compact or cluster-like. This is especially true in case of electro-magnetic showers. Hadronic showers produce broader and more diffuse images and especially at low energies, the light distribution can lose its compactness, resulting in unclustered images. Triggers induced by night-sky background are randomly distributed over the camera and thus naturally produce unclustered images. Thus, an image with no cluster at all is very likely to be due to night-sky background light or a hadron induced air shower.

Therefore, images containing no cluster at all are rejected. With the amplitude threshold at $A=3$ ph.e. and the multiplicity threshold at $N=4$ this condition reduces the transmission rate to the DAQ from 5 kHz to 3.3 kHz. Due to the lower amplitude threshold A , the γ -ray efficiency is improved (as compared to $A=5$ ph.e.) but the clustering condition also rejects γ -rays at lower energies. As illustrated in Figure 4, the overall gain of these two effects is positive and results in an improved detection efficiency at low energies and a lower energy threshold. Furthermore, only unclustered γ -ray events are rejected. These are events that would be very difficult to analyze using standard methods. Thus, the clustering condition allows to optimize the detector

Figure 4: Differential γ -ray count rate (arbitrary units) for the VLCT in monoscopic mode. The solid line represents the operation with amplitude threshold $A=5$ ph.e. and multiplicity $N=4$ (at 2.5 kHz). The dotted line shows the count rate for a reduced amplitude threshold ($A=3$ ph.e., $N=4$). The dashed line was obtained using a reduced amplitude threshold and activating the clustering condition.

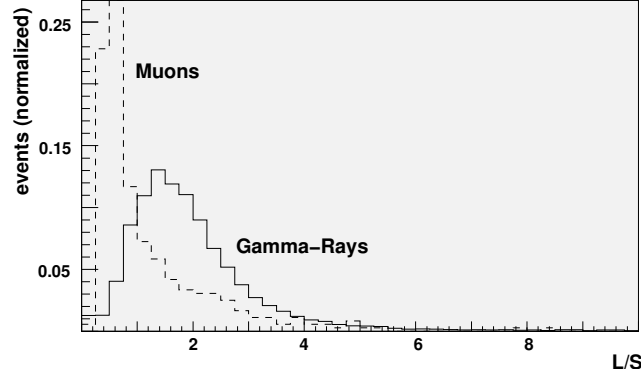


performance at low energies and to pre-select high-quality images for the analysis.

3.2 L2 Hillas analysis and L/S Condition

The width W and length L (second moment analysis, Hillas parameters) of the shower image are typically used in Cherenkov telescope analyses to separate electro-magnetic from hadron induced air showers. Towards lower energies the separation quality tends to decrease. Between a few tens of GeV and 100 GeV our simulations yield a very bad separation power of these parameters. A criterium which is often used in monoscopic Cherenkov telescope analyses for muon-rejection is the Length over Size (L/S) parameter. In Figure 5, the distribution of the L/S parameter is shown for γ -rays simulated with a Crab-Nebula like spectrum and muons. If a cut is chosen such as to keep 95 % of all γ -rays, 50 % of all muons are rejected. This rejection quality is reduced to ≈ 30 % if instead of the full amplitude information S the pseudo size PS is used. If the SPS amplitude information is used, the rejection factor drops to less than 20 %.

Figure 5: L/S parameter distribution for simulated muons and γ -rays (simulated with a Crab-Nebula like spectrum).



4 Conclusions

First studies of rejection criteria for a second level trigger for H.E.S.S. phase II have been made. The results show that even with the simplest rejection criteria it is possible to reduce the trigger rate of the planned additional very large central telescope. At the same time, the efficiency for γ -rays can be improved at low energies and the energy threshold can be reduced, thus optimizing the data-flow and the detector performance.

Acknowledgments

The support of the Namibian authorities and of the University of Namibia in facilitating the construction and operation of H.E.S.S. is gratefully acknowledged, as is the support by the German Ministry for Education and Research (BMBF), the Max Planck Society, the French Ministry for Research, the CNRS-IN2P3 and the Astroparticle Interdisciplinary Programme of the CNRS, the U.K. Particle Physics and Astronomy Research Council (PPARC), the IPNP of the Charles University, the South African Department of Science and Technology and National Research Foundation, and by the University of Namibia. We appreciate the excellent work of the technical support staff in Berlin, Durham, Hamburg, Heidelberg, Palaiseau, Paris, Saclay, and in Namibia in the construction and operation of the equipment.

References

- [1] Goret, P., “SAM a new ASIC for the front-end emlectronics of HESS II ”, *these proceedings pp. 501-507*
- [2] Hartman, R. C., Bertsch, S. D., Bloom, A. W., et al., ApJ Supplement, **123**, 79 (1999)
- [3] Hillas, A. M., 19th International Cosmic Ray Conference, **3**, 445 (1985)
- [4] Punch, M., “H.E.S.S. Phase II”, *these proceedings pp. 379-391*
- [5] Funk, S., Hermann, G., Hinton, J., et al. Astropart.Phys. **22**, 285 (2004)

